Supporting Information

Kanter et al. 10.1073/pnas.1111600109

SI Materials and Methods

Studies on Preexisting Advanced Atherosclerotic Lesions and Lesions in Severely Hyperlipidemic Mice. To investigate the effect of diabetes and myeloid-selective long-chain acyl-CoA synthetase 1 (ACSL1) deficiency on advanced preexisting lesions, female low-density lipoprotein receptor $(LDLR)^{-/-}$; glycoprotein (GP) mice (12–14 wk old) were fed a high-fat semipurified diet (1) for 15 wk to allow advanced lesions to develop in the brachiocephalic artery (BCA). The mice were then switched to the low-fat diet and transplanted with bone marrow from WT or $ACSL1^{M-/-}$ mice; 4 wk after the bone marrow transplant, diabetes was induced using lymphocytic choriomeningitis virus (LCMV). The mice were maintained after onset of diabetes for another 12 wk. At the end of the study, the BCA was dissected, embedded, and serial-sectioned. Every fourth section was stained using a Movat's pentachrome stain as described previously, and adjacent sections were used for immunohistochemistry (1). All measurements and scoring were done by an investigator in a masked fashion. All Movat's pentachrome-stained BCA sections were scored for the absence or presence of medial glycosaminoglycans, collagen, calcification and chondrocyte-like cells, and lesion collagen, cholesterol clefts, necrotic core, chondrocyte-like cells, calcification, and intraplaque hemorrhage as described previously (1, 2). A severity index score was calculated as the sum of the frequencies of the following characteristics throughout the entire BCA: collagen (medial and intimal), calcification and chondrocyte-like cells (medial and intimal), cholesterol clefts, necrotic core, and intraplaque hemorrhage. Sections adjacent to the maximal lesion site were used to measure necrotic core areas. Plasma levels of triglycerides and nonesterified fatty acids were determined using colorimetric assays from Sigma Aldrich and WAKO, respectively.

To evaluate the effect of myeloid ACSL1 deficiency in a hyperlipidemic insulin-resistant model, male $LDLR^{-/-}$ mice were transplanted with WT or ACSL1-deficient bone marrow, allowed to recover for 3 wk, and then fed a diet rich in saturated fat and carbohydrates (DDC) as previously described (3) for an additional 24 wk. At the end of the study, the extent of atherosclerosis was determined in the BCA, aorta (en face), and aortic sinus. Aortic sinus lesions were measured on three separate sections (all around the site where all three leaflets were present) and averaged within each animal.

Measurements of Neutral Lipids. Thioglycollate-elicited macrophages or bone marrow-derived macrophages were harvested and in some experiments, were stimulated with BSA alone or different concentrations of BSA-bound 18:1 or 50 μg/mL acetylated LDL for 24 or 48 h. Subsequently, lipids were extracted using chloroform/methanol, dried down, and resuspended in 100% ethanol followed by colorimetric analysis of total triacylglycerol (TG) (Sigma Aldrich). To measure total cholesterol, unesterified cholesterol, and cholesteryl esters, the Amplex Red assay (Invitrogen) was used. Results were confirmed by analyzing [^{3}H]-cholesterol distribution in the cholesteryl ester (CE) and free cholesterol pool after a 24-h loading with 50 μg/mL acetylated LDL and [^{3}H] cholesterol (1 mCi/mL; NEN Life Science Products). Uptake of acetylated LDL was evaluated by stimulating macrophages in the presence of 50 μg/mL acetylated LDL and [^{3}H]-cholesterol (1 mCi/mL) for 24 h. The cells were washed and lysed in 1 M NaCl, and the accumulated cellular radioactivity was analyzed by scintillation counter and normalized to cellular protein levels. Nonesterified fatty acids were analyzed in cell lysates using an assay from WAKO. For microscopic evaluation of intracellular neutral lipid droplets, macrophages were fixed using 10% neutral buffered formalin (Sigma-Aldrich) followed by oil red O staining for 20 min. The cells were counterstained using Harris hematoxylin (Sigma Aldrich) for 10 min.

Flow Cytometry and Real-Time PCR Analysis of Blood Cells. For flow cytometric analysis of monocyte numbers and subsets, blood cells were separated from plasma, and erythrocytes were lysed. The method described by Tacke et al. (4) was used. In short, the remaining white blood cells were counted and incubated with an FC blocker (CD16/32; eBiosciences). The cells were then incubated with a mixture of monoclonal antibodies against T cells (CD90.2-Rphycoerythrin (PE), 53–2.1), B cells (B220-PE, RA3-6B2), NK cells (CD49b-PE, DX5 and NK1.1-PE, PK136), granulocytes (Ly6G-PE, 1A8), myeloid cells (CD11b-APC, M1/70), and monocytes subsets (Ly6C-FITC, AL-21). All antibodies were purchased from eBioscience with the exception of Ly6 markers (BD Biosciences). The cells were then sorted on a flow cytometer (Cytopeia). Monocytes were gated based on side $scatter^{lo}$ forward $scatter^{hi}$ $CD11b^+CD90.2^-B220^-Cd49b^-Nk1.1^-Ly6G^-$ [allophycocyanin $(APC)^+PE^-$]. The monocytes were then analyzed for Ly6C levels. Neutrophil numbers were estimated from the APC^+ PE^+ pool.

For real-time PCR, blood cells were separated from plasma, and erythrocytes were lysed. The remaining pellet was resuspended in RLT buffer (Qiagen) and frozen until use. RNA was extracted and reverse transcribed followed by real-time quantitative PCR for *S100a8* (primarily expressed in neutrophils).

Fatty Acid Preparation for Cell Stimulation. Sodium salts of fatty acids (Nu-Check Inc.) were prepared in sterile, endotoxin-free water. At the day of the experiment, fatty acids were added to a final concentration of 70 or 225 μM in 0.5% fatty acid-free/endotoxin-free BSA containing endotoxin-free RPMI, which results in ∼1:1 and 3:1 ratios of fatty acids to BSA, respectively. The fatty acids were then allowed to equilibrate with the BSA for 1 h at 37 °C before addition to macrophages. Endotoxin contamination was ruled out in all solutions exposed to the cells using a chromogenic endpoint LAL assay from Invitrogen. Endotoxin levels were below 50 pg/mL.

[^{14}C]-18:1 Partitioning into Neutral Lipids and Acid-Soluble Metabolites. Partitioning of acyl-CoAs into intracellular lipid pools was analyzed by TLC as described previously (5), and acid soluble metabolites in the conditioned media were used as an index of β-oxidation (6).

1. Johansson F, et al. (2008) Type 1 diabetes promotes disruption of advanced atherosclerotic lesions in LDL receptor-deficient mice. *Proc Natl Acad Sci USA* 105:2082–2087.
2. Renard CB, et al. (2004) Diabetes and diabetes-associated lipid abnormalities have distinct effects on initiation and progression of atherosclerotic lesions. *J Clin Invest* 114:659–668.
3. Subramanian S, et al. (2008) Dietary cholesterol worsens adipose tissue macrophage accumulation and atherosclerosis in obese LDL receptor-deficient mice. *Arterioscler Thromb Vasc Biol* 28:685–691.
4. Tacke F, et al. (2007) Monocyte subsets differentially employ CCR2, CCR5, and CX3CR1 to accumulate within atherosclerotic plaques. *J Clin Invest* 117:185–194.
5. Askari B, et al. (2007) Rosiglitazone inhibits acyl-CoA synthetase activity and fatty acid partitioning to diacylglycerol and triacylglycerol via a peroxisome proliferator-activated receptor-γ-independent mechanism in human arterial smooth muscle cells and macrophages. *Diabetes* 56:1143–1152.
6. Lewin TM, Wang S, Nagle CA, Van Horn CG, Coleman RA (2005) Mitochondrial glycerol-3-phosphate acyltransferase-1 directs the metabolic fate of exogenous fatty acids in hepatocytes. *Am J Physiol Endocrinol Metab* 288:E835–E844.

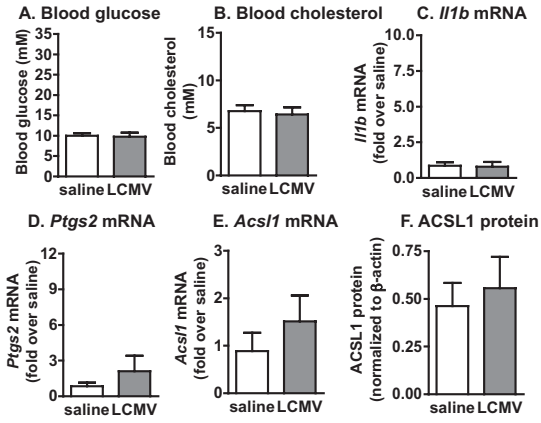

Fig. S1. LCMV injection in the absence of the GP transgene does not induce an inflammatory macrophage phenotype or ACSL1. LDLR$^{-/-}$ mice without the GP transgene (n = 4–5) were injected with LCMV or saline. All mice were maintained on a low-fat diet for 4 wk after LCMV injection like in Fig. 1. At the end of 4 wk, blood glucose (*A*) and blood cholesterol (*B*) were measured, and thioglycollate-elicited peritoneal macrophages were harvested by lavage. Real-time PCR was used to determine abundance of (*C*) *Il1b* mRNA, (*D*) prostaglandin-endoperoxide synthase 2 mRNA, and (*E*) *Acsl1* mRNA. (*F*) ACSL1 protein determined by Western blot. The results are expressed as mean + SEM.

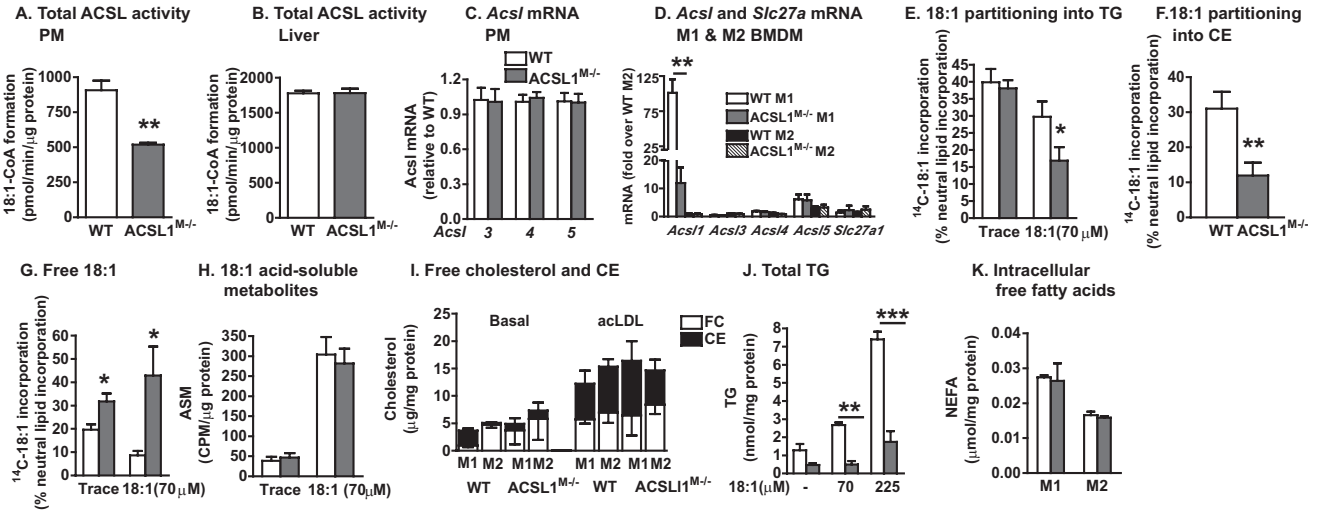

Fig. S2. *Acsl* and *Slc27a1* (*Fatp1*) levels and fatty acid partitioning in WT and ACSL1-deficient macrophages. Total ACSL1 activity was determined in WT and ACSL1$^{M-/-}$ thioglycollate-elicited macrophages (*A*) and liver (*B*). Real-time PCR was used to determine the abundance of ACSL isoforms in thioglycollate-elicited macrophages (*C*; n = 6) or bone marrow-derived macrophages polarized to M1 and M2 (*D*). Thioglycollate-elicited macrophages from WT and ACSL1$^{M-/-}$ mice were stimulated with trace amounts of [^{14}C]-18:1 alone or with 70 μM 18:1 or 50 μg/mL acetylated LDL for 48 h;, and lipids were extracted and separated (*E*–*G*); 18:1 partitioning into TG (*E*), CEs (*F*), and free 18:1 (*G*) was quantified and expressed as percent of total neutral lipid incorporation (n = 8). (*H*) β-Oxidation was measured as described in *Materials and Methods*. (*I*) ACSL1$^{M-/-}$ and WT bone marrow-derived macrophages (BMDMs) were activated into M1 or M2 and stimulated with acetylated LDL (50 μg/mL), and cholesterol was measured using an Amplex Red assay. (*J*) Total TG was measured after 48 h of incubation with indicated amounts of 18:1. (*K*) Intracellular nonesterified fatty acids (NEFA) were measured using a colorimetric assay. Results are expressed as mean + SEM; n = 3 unless otherwise stated. *P < 0.05, **P < 0.01, and ***P < 0.001 by Student t test or one-way ANOVA. PM, peritoneal macrophages.

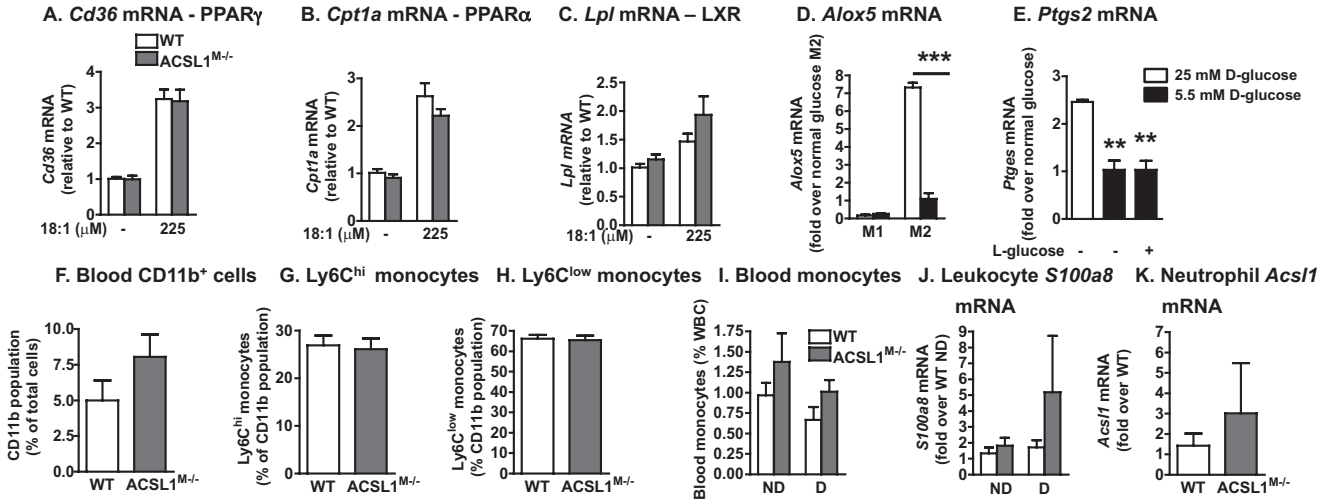

Fig. S3. Potential mechanisms. Thioglycollate-elicited macrophages were collected and adherence-purified followed by a 24-h stimulation with 18:1. Levels of mRNA for peroxisome proliferator-activated receptors or liver X receptor downstream target genes were analyzed using real-time PCR (*A*–*C*; $n = 6$). (*D*) Arachidonate 5-lipoxygenase mRNA in WT M1 and M2 macrophages under normal (5.5 mM) and high- (25 mM) glucose conditions was measured by real-time PCR. (*E*) Prostaglandin-endoperoxide synthase 2 mRNA in WT M1 macrophages differentiated under high D-glucose (25 mM), normal D-glucose (5.5 mM), or normal D-glucose (5.5 mM) + L-glucose (19.5 mM) osmotic control. Whole blood was taken from WT and ACSL1$^{M-/-}$ mice (*F*–*H*; $n = 4$–8), nondiabetic or diabetic WT and ACSL1$^{M-/-}$ mice 4 wk after induction of diabetes by streptozotocin (*I*; $n = 3$–4), or diabetic or nondiabetic mice transplanted with bone marrow from WT and ACSL1$^{M-/-}$ mice (*J*; $n = 3$–10). Erythrocytes were lysed, and the remaining leukocytes were analyzed or stained using antibodies described in *Materials and Methods*. (*F*) Number of CD11b$^+$ cells (a measure of monocytes) was based on the scatter^{lo} forward scatter^{hi} CD11b$^+$CD90.2$^-$B220$^-$Cd49b$^-$Nk1.1$^-$Ly6G$^-$ (APC$^+$PE$^-$) population followed by gating based on Ly6C expression (*G* and *H*). (*I*) Monocytes as percent of leukocytes were estimated by using the EasySep Mouse Monocyte Enrichment kit (Stemcell Technologies. (*J*) Real-time PCR was used to determine abundance of *S100a8* mRNA (primarily expressed in neutrophils (1). (*K*) Neutrophils were isolated from the peritoneal cavity 4 h after thioglycollate injection and subjected to adhesion purification. Nonadherent cells were used for analysis of *Acsl1* mRNA levels ($n = 3$). The results are expressed as mean + SEM ($n = 3$ unless otherwise stated). $^{**}P < 0.01$ and $^{***}P < 0.001$ by one- or two-way ANOVA.

1. Averill MM, et al. (2011) S100A9 differentially modifies phenotypic states of neutrophils, macrophages, and dendritic cells: Implications for atherosclerosis and adipose tissue inflammation. *Circulation* 123:1216–1226.

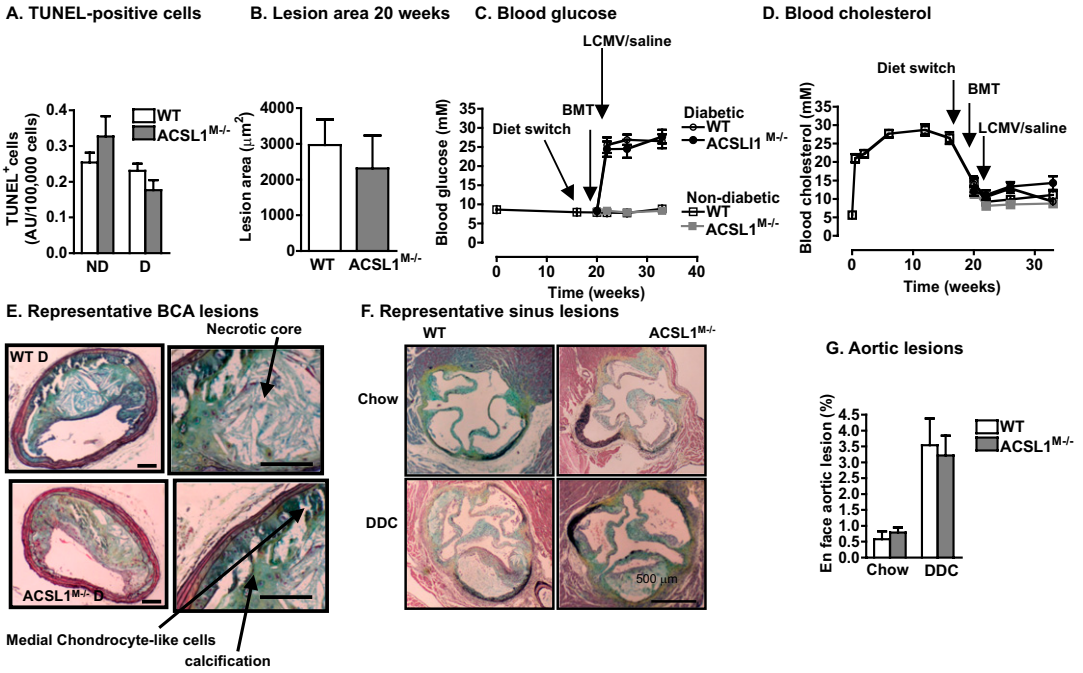

Fig. S4. Myeloid ACSL1 deficiency reduces advanced atherosclerotic lesion severity in diabetic mice. Thioglycollate-elicited macrophages from nondiabetic and diabetic mice 4 wk after induction of diabetes by streptozotocin were harvested and analyzed for apoptosis using a TUNEL assay (*A*). Nondiabetic female LDLR$^{-/-}$;GP^{+} mice (12–14 wk) were transplanted with WT or ACSL1$^{M-/-}$ bone marrow, allowed to recover, and then switched to the same low-fat diet shown in Fig. 5 and maintained for 20 wk. Lesion size in BCA (*B*). Female LDLR$^{-/-}$;GP^{+} mice were fed a high-fat diet for 16 wk and then switched to the low-fat diet. One week after the diet switch, the mice were bone marrow-transplanted with bone marrow from WT or ACSL1$^{M-/-}$ mice. After a 3-wk recovery period, diabetes was induced. The mice were then fed the low-fat diet for an additional 12 wk, and blood glucose (*C*) and cholesterol (*D*) were monitored at the indicated time points (n = 17–26). At the end of the study, the entire BCA was serial-sectioned. (*E*) Examples of Movat's pentachrome-stained cross-sections of the BCA from a diabetic mouse that had received bone marrow from a WT mouse and a diabetic mouse that had received bone marrow from an ACSL1$^{M-/-}$ mouse. The results in *C* and *D* are expressed as mean ± SEM (n = 16–26). (Scale bars: 100 μm; magnified photos, 20 μm.) (*F* and *G*) LDLR$^{-/-}$ mice were fed a DDC for 24 wk. At the end of the study, there were no differences in lesion area in the sinus (*F*) or aorta (*G*) between mice with WT and ACSL1$^{M-/-}$ bone marrow, although the high-fat diet had a significant effect. Mice fed DDC also had significantly elevated blood cholesterol levels compared with chow-fed mice (chow WT = 7.3 ± 0.3 mM cholesterol, chow ACSL1$^{M-/-}$ = 7.3 ± 0.4 mM, DDC WT = 37.5 ± 0.4 mM, and DDC ACSL1$^{M-/-}$ = 37.9 ± 4.6 mM; both DDC $P < 0.05$ vs. chow). Results are expressed as mean ± SEM (n = 8–13).

Table S1. Effects of glucose and ACSL1 deficiency on lipid mediators in M1 macrophages

Lipid mediator (pg/6 × 10^6 cells)	WT 25 mM glucose	ACSL1$^{M-/-}$ 25 mM glucose	WT 5 mM glucose	ACSL1$^{M-/-}$ 5 mM glucose
5-HETE	1,698 ± 91	1,833 ± 86	1,333 ± 45	1,208 ± 255
12-HETE	5,866 ± 199	6,436 ± 139	5,698 ± 316	4,761 ± 856
15-HETE	3,118 ± 140*	3,014 ± 94*	1,793 ± 202	1,672 ± 298
14-HDHA	869 ± 38	900 ± 11	786 ± 36	738 ± 150
17-HDHA	287 ± 18*	307 ± 22†	166 ± 30	160 ± 35
PGD_2	19,155 ± 831‡,¶	14,446 ± 1,907*	7,667 ± 353	6,597 ± 751
$PGF_{2\alpha}$	4,749 ± 269*	4,055 ± 554*	2,324 ± 318	1,750 ± 215
LTB_4	31 ± 4	28 ± 3	19 ± 2	20 ± 1
18-HEPE	93 ± 3	100 ± 3	73 ± 4	72 ± 9

Maresin 1, protectin 1, resolvin D1, 20-OH-LTB_4, lipoxin A_4, lipoxin B_4, resolving E1, and resolving E2 were nondetectable in all samples. Results expressed as mean ± SEM; n = 4–5.

*$P < 0.01$ compared with the same genotype in 5 mM glucose.

$^{\dagger}P < 0.05$ compared with the same genotype in 5 mM glucose.

$^{\ddagger}P < 0.001$ compared with the same genotype in 5 mM glucose.

$^{\P}P < 0.05$ compared with ACSL1$^{M-/-}$ in the same glucose (one-way ANOVA).

Table S2. Myeloid ACSL1 deficiency does not significantly affect circulating levels of free fatty acids, IL-6, or SAA

	Nondiabetic		Diabetic	
	WT (n = 14)	ACSL1$^{M-/-}$ (n = 12)	WT (n = 15)	ACSL1$^{M-/-}$ (n = 10)
NEFA (mM)	0.20 ± 0.02	0.19 ± 0.03	0.24 ± 0.05	0.24 ± 0.03
IL-6 (pg/mL)	4.0 ± 0.8	2.5 ± 1.7	12.2 ± 6.7	13.5 ± 5.5
SAA (μg/mL)	14.0 ± 1.5	13.0 ± 1.0	311 ± 170	110.5 ± 77.6

Table S3. Myeloid ACSL1 deficiency confers a small reduction of the severity of preexisting advanced atherosclerotic lesions in diabetic mice

	ND WT (n = 26)	ND ACSL1$^{M-/-}$ (n = 23)	D WT (n = 19)	D ACSL1$^{M-/-}$ (n = 16)
Body weight (g)*	23.1 ± 2.5	23.8 ± 2.4	18.1 ± 1.7†	17.3 ± 2.2†
Triglycerides (mM)	0.99 ± 0.08	1.0 ± 0.08	1.5 ± 0.3	1.3 ± 0.2
NEFA (mM)	0.31 ± 0.03	0.31 ± 0.02	0.30 ± 0.06	0.26 ± 0.03
Plasma IL-6 (pg/mL)	6.9 ± 2.5	8.4 ± 1.8	10.4 ± 2.2	10.4 ± 3.4
Lesion area (μm^2)	130,234 ± 11,116	131,594 ± 13,285	142,002 ± 11,205	116,907 ± 17,167
Necrotic core area (μm^2)	28,022 ± 5,568	19,350 ± 4,637	17,335 ± 3,186	21,632 ± 4,233
SM α-actin area (μm^2)	0.003 ± 0.001	0.002 ± 0.001	0.003 ± 0.001	0.007 ± 0.004
Mac-2 area (μm^2)	8,306 ± 1,382	13,333 ± 2,617	11,425 ± 2,523	10,440 ± 1,703
Lesion severity index‡	331 ± 27	259 ± 29	270 ± 22	222 ± 22†
Cholesterol clefts (%)	63.8 ± 6.4	52.0 ± 7.5	63.5 ± 6.3	48.1 ± 7.0
Necrotic core (%)	46.6 ± 6.7	41.0 ± 6.1	45.4 ± 5.2	35.6 ± 6.1
Lesion chondrocyte-like cells (%)	64.8 ± 6.5	55.0 ± 8.0	52.3 ± 8.3	47.4 ± 8.0
Lesion calcification (%)	47.0 ± 7.4	34.6 ± 7.2	36.1 ± 7.9	30.2 ± 6.4
Intraplaque hemorrhage (%)	13.0 ± 3.7	7.7 ± 4.5	6.2 ± 2.9	12.5 ± 4.9
Medial collagen (%)	60.9 ± 5.7	46.1 ± 6.9	47.2 ± 6.3	39.6 ± 5.4†
Medial chondrocyte-like cells (%)	22.2 ± 5.4	17.2 ± 5.5	13.5 ± 4.0	6.2 ± 3.2†
Medial calcification (%)	12.9 ± 3.9	5.2 ± 2.6	5.6 ± 2.8	2.3 ± 1.3

ND, nondiabetic; D, diabetic.

*$P < 0.001$ comparing nondiabetic and diabetic by two-way ANOVA.

$^{\dagger}P < 0.05$ compared with nondiabetic WT by one-way ANOVA.

$^{\ddagger}P < 0.05$ comparing WT and ACSL1 $^{M-/-}$ by two-way ANOVA.